

Diet-induced prediabetes: Effects on the activity of the renin–angiotensin–aldosterone system in selected organs

Bongeka Cassandra Mkhize^{1*} , Palesa Mosili¹, Phikelelani Sethu Ngubane¹, Ntethelelo Hopewell Sibiya², Andile Khathi¹

¹University of KwaZulu-Natal, Durban, South Africa, and ²Rhodes University, Grahamstown, South Africa

Keywords

Hyperglycemia, Prediabetes, Renin–angiotensin–aldosterone system

*Correspondence

Bongeka Cassandra Mkhize
 Tel.: +27-31-260-7585
 Fax: +27-31-260-7132
 E-mail address:
 bongeka.mkhize28@gmail.com;
 215032519@stu.ukzn.ac.za

J Diabetes Investig 2022; 13: 768–780

doi: 10.1111/jdi.13690

ABSTRACT

Aims/Introduction: Derangements often observed with type 2 diabetes are associated with disturbances in renin–angiotensin–aldosterone system (RAAS) activity. A positive correlation between local RAAS activity and the complications observed in type 2 diabetes has been noted. However, the detrimental ramifications due to moderate hyperglycemia noted in prediabetes, and the affected organ system and mechanistic pathways are not elucidated. Hence, this study investigated the effects of diet-induced prediabetes on RAAS in various organs.

Materials and Methods: Male Sprague–Dawley rats were separated into two groups: (i) non-prediabetes through exposure to standard rat chow group; and (ii) diet-induced prediabetes group by exposure to a high-fat high-carbohydrate diet for 32 weeks. RAAS activity in the skeletal muscle, adipose tissue, liver, pancreas and heart was determined through the analysis of RAAS components, such as renin, angiotensinogen, angiotensin-converting enzyme and angiotensin II type 1 receptor through polymerase chain reaction, as well as the quantification of angiotensin II and aldosterone concentration. Furthermore, nicotinamide adenine dinucleotide phosphate oxidase, superoxide dismutase and glutathione peroxidase 1 concentrations were determined in the skeletal muscle, pancreas and heart, in addition to the hepatic triglycerides.

Results: The RAAS components were elevated in the diet-induced prediabetes group when compared with the non-prediabetes group. This was further accompanied by increased nicotinamide adenine dinucleotide phosphate oxidase and reduced superoxide dismutase and glutathione peroxidase 1 concentrations in the selected organs, in addition to the elevated hepatic triglycerides concentration in the diet-induced prediabetes by comparison to non-prediabetes group.

Conclusions: Due to these observed changes, we suggest that local RAAS activity in the prediabetes state in selected organs elicits the derangements noted in type 2 diabetes.

INTRODUCTION

A positive correlation has been found between the increased consumption of high caloric diets and the increased prevalence of type 2 diabetes. Type 2 diabetes is a chronic metabolic disorder that is characterized by dyslipidemia, oxidative stress, hypertension and insulin resistance¹. These derangements of type 2 diabetes have been evidenced to be associated with the alterations in various organ systems, such as the renin–angiotensin–aldosterone system (RAAS)².

The RAAS is a regulatory signaling system that maintains blood pressure through the regulation of fluid and electrolyte homeostasis³. In type 2 diabetes, the changes in systemic RAAS leading to various detrimental effects, such as hypertension, cardiovascular dysfunction and renal failure, have been well documented^{4–6}. Additionally, alterations in organ-specific RAAS have been evidenced in various tissues, such as the adipose, pancreas, liver, skeletal muscle, kidney and heart, in type 2 diabetes^{2,7,8}. In the pancreas, RAAS is in the acinar and islet cells, whereby acinar RAAS maintains exocrine function and islet RAAS conversely contributes to glucose homeostasis by

Received 6 July 2021; revised 14 September 2021; accepted 4 October 2021

regulating glucose-induced insulin secretion⁹. Interestingly, in type 2 diabetes, the activity of this system in the pancreatic β -cells has been linked to insulin insufficiency and insulin resistance in the adipose tissue¹⁰. Organ-specific RAAS in the adipose tissue alters the cell differentiation contributing to obesity, which was reported to affect 28.3% of adults in 2016^{11,12}. The RAAS in adipose tissue also limits the adipose buffering capacity, hence ectopic triglyceride distribution to the pancreas, skeletal muscle and the liver¹³. This further causes hypertriglyceridemia, insulin resistance and diabetic dyslipidemia in the liver¹⁴. The activity of RAAS in the skeletal muscle has been suggested to affect the insulin signaling pathway, and this has been postulated to contribute to increased caloric intake and bodyweight in addition to the development of type 2 diabetes¹⁵. However, the activity of RAAS in the kidney and heart dysregulates the morphology and function of these organs, resulting in dysregulations in blood pressure, as well as electrolyte and fluid balance^{16,17}.

Studies showed that the onset of type 2 diabetes is often preceded by prediabetes, which is an intermediary stage that is characterized by moderate insulin resistance and impaired glucose tolerance¹⁸. Prediabetes is an asymptomatic stage that can span a period of several years, hence, it is not easily diagnosed¹⁹.

Although there is substantial evidence of local RAAS activity in type 2 diabetes, there is a paucity in the literature of the organ-specific changes that occur during the prediabetes state. Using a diet-induced prediabetes animal model, the present study aimed to explore organ-specific changes in RAAS activity during the prediabetes state.

METHODS AND MATERIALS

Animals and housing

The study used male Sprague–Dawley rats (weight 150–180 g) produced and housed at the University of KwaZulu-Natal Biomedical Research Unit, Durban, South Africa. The animals were housed under conventional laboratory settings, which included a constant temperature of 22°C, a CO₂ concentration of 5,000 p.p.m., a relative humidity of 55 ± 5% and illumination (12-h light/dark cycle, lights on at 07.00 hours). As mentioned by Luvuno *et al.*, the noise level was kept at 65 dB²⁰. The animals were allowed access to food and fluids *ad libitum*. The Animal Research Ethics Committee at the University of KwaZulu-Natal (ETHICS#: AREC/086/018D) approved all animal experiments. Before being exposed to the experimental diets, the animals were permitted to acclimate to their new habitat for 1 week while eating standard rat chow and drinking tap water²¹. Procedures involving animal care were carried out in accordance with the institutional guidelines for animal care of the University of KwaZulu-Natal, which adhere to the principles and guidelines of the Canadian Council on Animal Care.

Induction of prediabetes

The animals were randomly assigned to the following diet groups: standard rat chow with normal drinking water (non-

prediabetes [NPD]; $n = 6$), and high-fat high-carbohydrate diet with drinking water supplemented with 15% fructose (high-fat high-carbohydrate + fructose, prediabetes [PD]; $n = 6$; AVI Products Pty Ltd, Waterfall, South Africa). Prediabetes was induced by allowing the animals to feed on the high-fat high-carbohydrate and fructose diet for 32 weeks as previously described²². After 32 weeks, the American Diabetes Association criteria were used to diagnose prediabetes, whereby the criteria to define prediabetes include impaired fasting glucose with fasting plasma glucose concentrations of 5.6–6.9 mmol/L, impaired glucose tolerance with a plasma glucose concentration of 7.8–11.0 mmol/L 2-h postprandial or glycated hemoglobin (HbA1c) of 5.7–6.4%. In the present study, the HbA1c was determined in whole blood, and the fasting plasma glucose concentration was determined with One-Touch select glucometer (Lifescan, Inverness, UK) at week 32. The animals that were fed the standard diet were also tested at week 32, and were found to be normoglycemic and without prediabetes. Furthermore, the animals were placed in individual metabolic cages (Tecniplast; Labotec, Cape Town, South Africa) overnight to determine caloric intake (food and water) and bodyweight (g).

Blood pressure measurements

The systolic, diastolic and mean arterial blood pressure (MAP) were measured at week 32 using the non-invasive tail-cuff method with photoelectric sensors (IITC Model 31 Computerized Blood Pressure Monitor; Life Sciences, Woodland Hills, CA, USA), as previously described (Luvuno *et al.*)²². The equipment was calibrated each day before measurements. The animals were kept warm at ±30°C in an enclosed chamber (IITC Model 303sc Animal Test Chamber; IITC Life Sciences, Woodland Hills, CA, USA) for 30 min before blood pressure recording. All measurements were carried out at 09.00 hours²³.

Blood collection and tissue harvesting

At the end of the trial, all animals were anesthetized for 3 min with isoflurane (100 mg/kg; Safeline Pharmaceuticals Pty Ltd, Roodeport, South Africa) administered in a gas anesthetic chamber (Biomedical Resource Unit, UKZN, Durban, South Africa)²¹. Blood was obtained from unconscious rats through heart puncture and then injected into separate pre-cooled heparinized containers. The blood was then centrifuged for 15 min at 4°C, 503 g (Eppendorf, Hamburg, Germany)²⁴. As previously stated by Luvuno *et al.*, plasma was collected and kept at –80°C in a Bio Ultra freezer (Snijders Scientific, Tilburg, the Netherlands) until biochemical analysis²². The tissues were rinsed and also stored at –80°C.

Biochemical analysis

The concentrations of nicotinamide adenine dinucleotide phosphate (NADPH) oxidase, superoxide dismutase (SOD) and glutathione peroxidase 1 (GPx1) in skeletal muscle, heart and pancreas, as well as plasma insulin, HbA1c, liver triglycerides (TGs) and endothelial nitric oxide synthase (eNOS) were

determined with separate, specialized enzyme-linked immunosorbent assay kits, as directed by the manufacturer (Elabscience and Biotechnology, Wuhan, China).

Angiotensin II in tissues

To avoid angiotensin II (Ang II) protease degradation, the adipose tissue, liver, pancreas, skeletal muscle and heart were washed in phosphate buffered saline to remove excess blood, snap frozen with liquid nitrogen and stored at -80°C . Frozen tissue samples were homogenized in 0.1% NHCl and 5% urastatin saline at 4°C . The homogenate was centrifuged for 30 min at 4°C at 10,000 g, with the supernatant collected and analyzed with an enzyme-linked immunosorbent assay²⁵.

Quantitative real-time polymerase chain reaction

Ribonucleic acid extraction in the skeletal muscle, adipose, pancreas, liver and heart were carried out as per the ReliaPrep miRNA Cell and Tissue Miniprep System (Promega, Madison, WI, USA). Reverse transcription reactions with 2 μg of total ribonucleic acid were used to make complementary deoxyribonucleic acids using the GoTaq[®] 2-Step RT-qPCR System as a complementary deoxyribonucleic acid synthesis kit (Promega), according to the manufacturer's instructions.

According to the manufacturer's instructions, the Roche light cycler SYBR Green I master mix was used for amplification on the (ROCHE LightCycler96 (Roche, Basel, Switzerland). (Table 1) lists the primer sequences (Metabion, Planegg, Germany) utilized in this investigation. The cycling conditions were: pre-incubation was carried out at 95°C for 60s, followed by a three-step amplification of 45 cycles at 95°C for 15 s, 60°C for 30 s and 72°C for 30 s. Melting was effectuated at 95°C for 10 s, 65°C for 60 s and 97°C for 1 s. Furthermore, cooling was achieved at 37°C for 30 s. Glyceraldehyde 3-phosphate dehydrogenase as an internal control was used to normalize the data to determine the relative expression of the gene of interest. Gene expression values are represented using the $2^{-\Delta\Delta\text{Ct}}$ method. The below primers were used.

Statistical analysis

All data are expressed as the mean \pm standard error of the mean. Statistical comparisons were carried out with GraphPad InStat software (version 5.00; GraphPad Software Inc., San Diego, CA, USA) using Student's unpaired two-sided *t*-test. A value of $P < 0.05$ was considered statistically significant.

RESULTS

Skeletal muscle RAAS components

The skeletal muscle renin, angiotensinogen (AGT), angiotensin-converting enzyme (ACE) and Ang II receptor type 1 (AT1R) relative expression in addition to the skeletal muscle Ang II and aldosterone protein concentration was analyzed at week 32. The results (Figure 1) showed that the relative expression of the renin, AGT, ACE and AT1R in addition to the protein concentration of the Ang II and aldosterone was significantly

TABLE 1 | List of primers used

Gene of interest	Sequence
Renin	Forward: 5'-GAGG-CCTTCCTTGACCAATC-3' Reverse: 5'-TGT-GAATCCCACAAGCAAG-3'
Angiotensinogen	Forward: 5'-GAGTGGGAGAGGTTCTC-AA-3' Reverse: 5'-TCGTAGATGCGAACAG-GA-3'
ACE	Forward: 5'-CCATCTGCTAGGGAA-CATGT-3' Reverse: 5'-GTGTCATCCCTG-CTTTATCA-3'
AT1R	Forward: 5'-GCTCACGTG-TCTCAGCAT-3' Reverse: 5'-TTGGCCAC-CAGCATCGT-3'
GAPDH	Forward: 5'-AGTGCCAGCCTCGTCTCATA-3' Reverse: 5'-GATGGTGATGGGTTCCCGT-3'

ACE, angiotensin-converting enzyme; AT1R, angiotensin II type 1 receptor; GAPDH, Glyceraldehyde 3-phosphate dehydrogenase.

($P < 0.05$), ($P < 0.01$) and ($P < 0.001$) increased in the PD group relative to the NPD group.

Fasting blood glucose, plasma insulin and HbA1c

The fasting blood glucose, plasma insulin and HbA1c concentration of the NPD and PD was measured at week 32. The results (Figure 2) showed that the fasting blood glucose, plasma insulin and HbA1c were significantly ($P < 0.01$, $P < 0.001$ and $P < 0.05$, respectively), higher in the PD group in comparison with the NPD group.

Caloric intake and bodyweight

The caloric intake and bodyweight in the NPD and PD were monitored at week 32. The results (Table 2) showed that the caloric intake and bodyweight were significantly ($P < 0.05$) and ($P < 0.05$) higher in the PD group in comparison with the NPD group.

Adipose tissue RAAS components

The adipose tissue renin, AGT, ACE and AT1R relative expression in addition to the Ang II and aldosterone concentration of the NPD and PD was measured at week 32. The results (Figure 3) showed that the relative expression of the RAAS components renin, AGT and AT1R was significantly ($P < 0.01$ and $P < 0.001$) increased in the PD group relative to the NPD group, whereas there was no statistical significance in ACE relative expression between both groups. Furthermore, there was no statistical significance in the Ang II and aldosterone concentration in the PD group in comparison with the NPD group.

Liver RAAS components

The liver renin, AGT, ACE and AT1R relative expression in addition to the protein concentration of Ang II and aldosterone of the NPD and PD were monitored at week 32. The results (Figure 4) showed that the renin, AGT, ACE and AT1R relative expression, and the protein concentration of the Ang II and aldosterone were significantly ($P < 0.05$, $P < 0.01$ and $P < 0.001$) higher in the PD group relative to the NPD group.

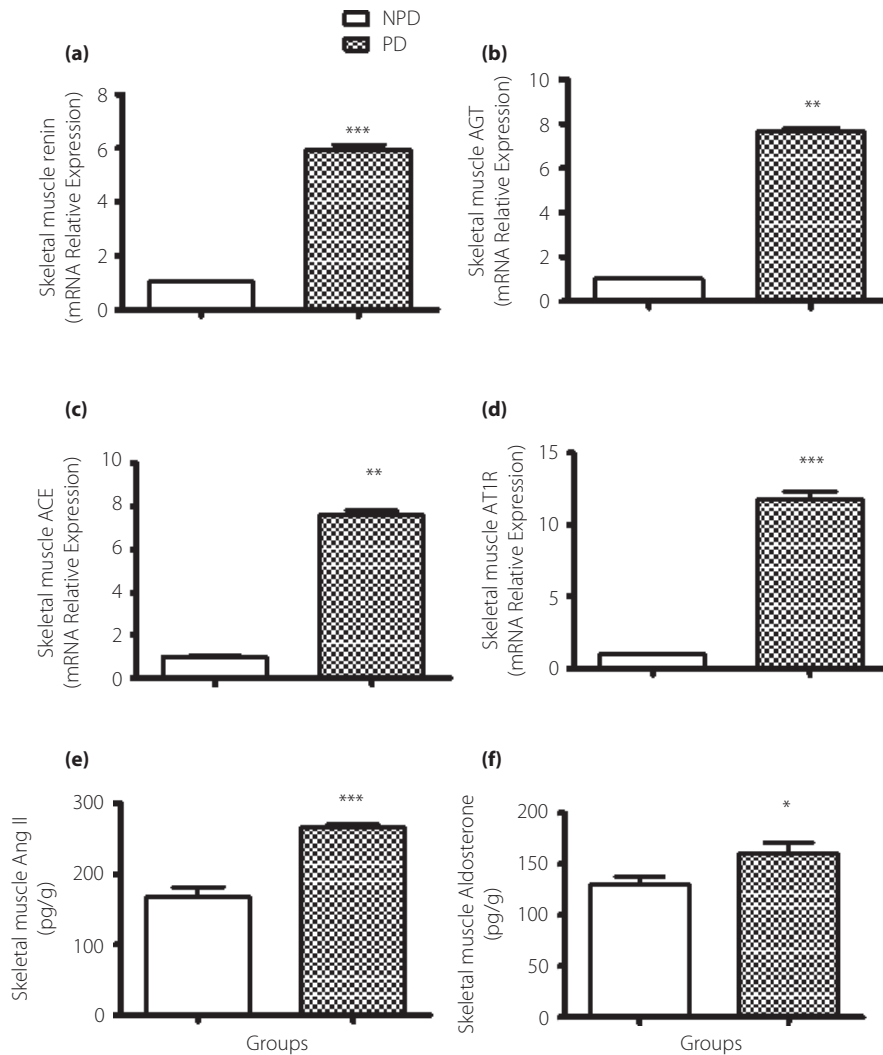


Figure 1 | The effects of a high-fat high-carbohydrate diet on the relative expression of the skeletal muscle renin–angiotensin–aldosterone system components, namely, (a) renin, (b) angiotensinogen (AGT), (c) angiotensin-converting enzyme (ACE), (d) angiotensin II type 1 receptor (AT1R), and the protein concentration of (e) angiotensin II (Ang II) and (f) aldosterone of rats at week 32. Values are presented as the means \pm standard error of the mean. * $P < 0.05$, ** $P < 0.01$ and *** $P < 0.001$ denotes significance relative to standard rat chow with normal drinking water (non-prediabetes [NPD]) diet-fed male Sprague–Dawley rats. mRNA, messenger ribonucleic acid; PD, prediabetes. (See the exact numerical values for figure 1 in table 4.1 in the supplementary information)

TG

The liver TG of the NPD and PD groups were analyzed at week 32. The results (Figure 5) showed a significant ($P < 0.001$) increase in liver TG in the PD group in comparison with the NPD group.

Pancreas RAAS components

The pancreas renin, AGT, ACE and AT1R relative expression, and the protein expression of the Ang II and aldosterone of the NPD and PD were measured at week 32. The results (Figure 6) showed that the relative expression of the RAAS components renin, AGT and AT1R was significantly ($P < 0.05$ and

$P < 0.01$) increased in the PD group relative to the NPD group, whereas there was no statistical significance in ACE relative expression between both groups. Furthermore, there was no statistical significance in the protein concentration of the Ang II and aldosterone at week 32.

eNOS and MAP

The eNOS and MAP of the NPD and PD groups were measured at week 32. The results (Figure 7) showed a significant ($P < 0.05$ and $P < 0.001$) increase in the eNOS concentration and MAP in the PD group in comparison with the NPD group.

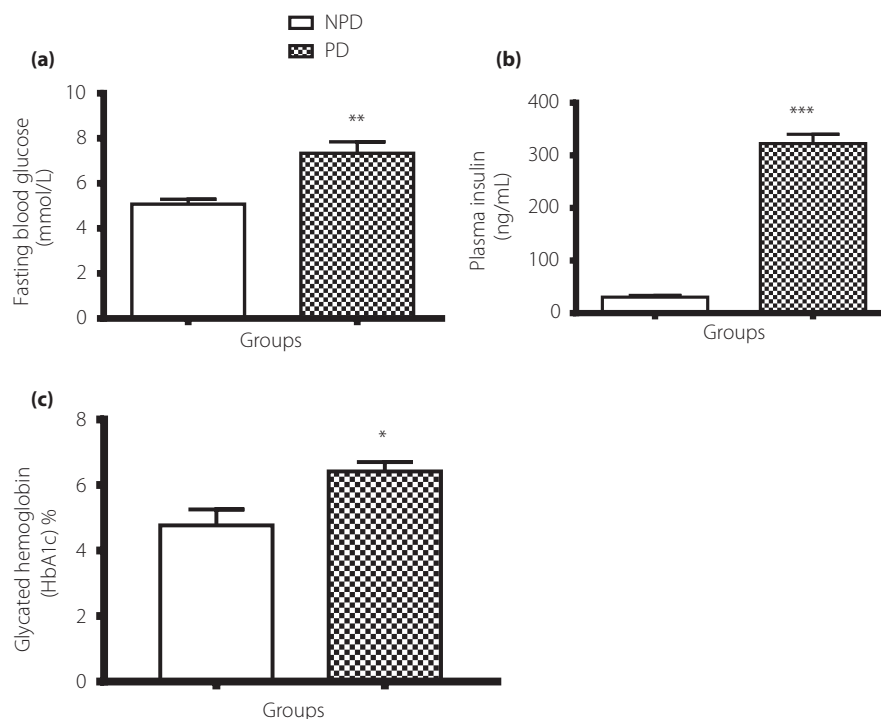


Figure 2 | The effects of a high-fat high-carbohydrate diet on the (a) fasting blood glucose, (b) plasma insulin and (c) glycated hemoglobin (HbA1c) of rats at week 32. Values are presented as the mean \pm standard error of the mean. ** $P < 0.01$, *** $P < 0.001$ and * $P < 0.05$ denotes comparison with standard rat chow with normal drinking water (non-prediabetes [NPD]) diet-fed male Sprague–Dawley rats. PD, prediabetes. (See the exact numerical values for figure 2 in table 4.2 in the supplementary information)

TABLE 2 | Effect of diet-induced prediabetes on the caloric intake and bodyweight in male Sprague–Dawley rats

	NPD	PD
Caloric intake (kcal/g)	210.6 \pm 12.9	462.5 \pm 17.4*
Bodyweight (g)	263.5 \pm 13.7	540.5 \pm 16.1*

Values are presented as the mean \pm standard error of the mean.

* $P < 0.05$. NPD, non-prediabetes; PD prediabetes.

Heart RAAS components

The heart renin, AGT, ACE and AT1R relative expression in addition to the protein concentration of Ang II and aldosterone of the NPD and PD were monitored at week 32. The results (Figure 8) showed that the relative expression of the renin, AGT, ACE and AT1R in addition to the protein concentration of Ang II and aldosterone was significantly ($P < 0.05$, $P < 0.01$ and $P < 0.001$) increased in the PD group relative to the NPD group.

Local RAAS oxidative stress markers

The skeletal muscle, pancreas, heart NADPH oxidase, SOD and GPx1 in the NPD and PD were monitored at week 32. The results (Table 3) showed that the NADPH oxidase

concentration was significantly ($P < 0.05$ and $P < 0.01$) higher in the PD group in comparison with the NPD, whereas the SOD and GPx1 were significantly ($P < 0.01$) lower in the PD in comparison with the NPD group.

DISCUSSION

Prediabetes is an asymptomatic state of chronic moderate hyperglycemia that precedes the onset of type 2 diabetes. A positive correlation between the development and progression of prediabetes, and the consumption of a high-fat, high carbohydrate diet was established in our laboratory²⁶. A plethora of information regarding the derangements associated with type 2 diabetes, such as the pathological activity of the RAAS in various organs, is well substantiated²⁷. However, local RAAS activity in the prediabetes stage and the mechanistic pathway in the development of prediabetes and progression to type 2 diabetes has not been elucidated. Hence, the present study investigated the role of diet-induced prediabetes in local RAAS in the skeletal muscle, adipose tissue, pancreas, liver and heart in the progression of prediabetes to type 2 diabetes.

The skeletal muscle is the primary organ for insulin-mediated glucose uptake²⁸. In type 2 diabetes, a positive correlation between hyperglycemia and local RAAS activity in the skeletal muscle has been noted²⁹. RAAS activity in the skeletal

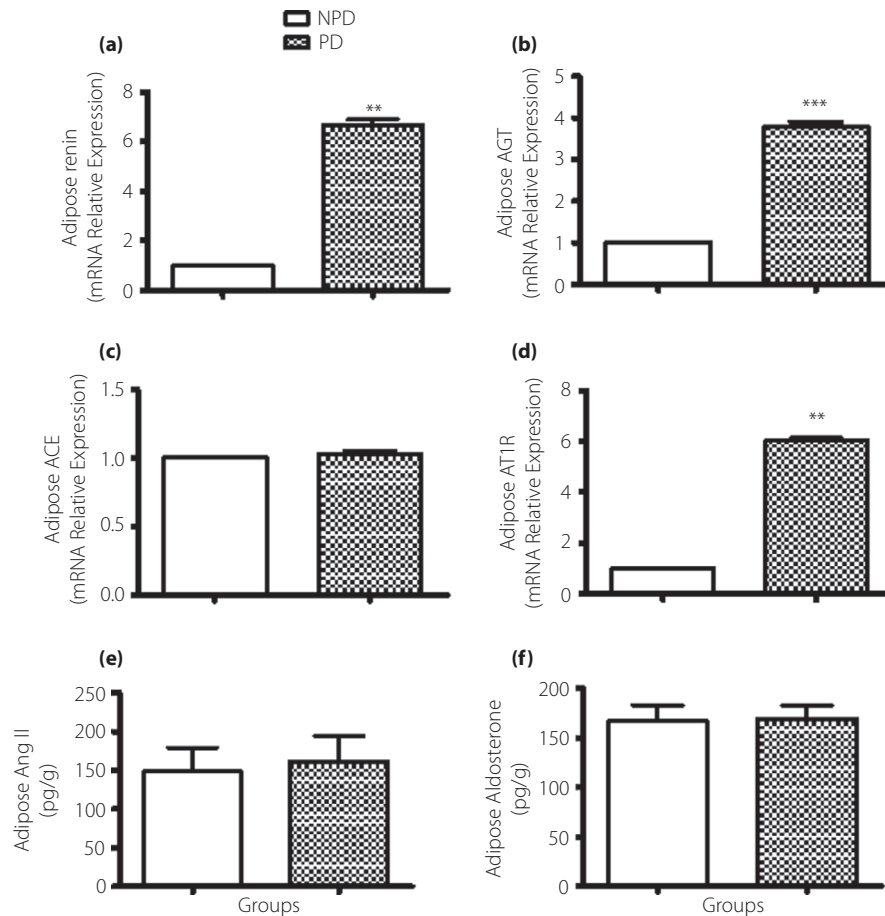


Figure 3 | The effects of a high-fat high-carbohydrate diet on the relative expression of the adipose tissue renin–angiotensin–aldosterone system components, namely, (a) renin, (b) angiotensinogen (AGT), (c) angiotensin-converting enzyme (ACE), (d) angiotensin II type 1 receptor (AT1R), and the protein concentration of (e) angiotensin II (Ang II) and (f) aldosterone of rats at week 32. Values are presented as the mean \pm standard error of the mean. ** $P < 0.01$ and *** $P < 0.001$, denotes significance relative to standard rat chow with normal drinking water (non-prediabetes [NPD]) diet-fed male Sprague–Dawley rats. mRNA, messenger ribonucleic acid; PD, prediabetes. (See the exact numerical values for figure 3 in table 4.3 in the supplementary information)

muscle has been shown to contribute to insulin resistance, whereby the Ang II/AT1 receptor binding inhibits the tyrosine phosphorylation of the insulin receptor substrate³⁰. Physiologically, the insulin and insulin receptor substrate-binding initiates the downstream effects of this pathway, which results in glucose uptake³¹. Interestingly, because of the hyperglycemia observed in type 2 diabetes, there is local RAAS activity, whereby the Ang II/AT1R receptor binding does not only contribute to insulin resistance through the inhibition of insulin/insulin substrate binding, but has been proven to promote the production of reactive oxygen species (ROS) through NADPH oxidase activity³².

In the present study, there was an increase in local RAAS and NADPH oxidase activity, whereby RAAS components were upregulated, thus enabling Ang II/AT1R interaction, which we postulate resulted in insulin resistance through the tyrosine inhibition and NADPH oxidase activation, which was observed

in this study. Various mechanisms regulate ROS, which include enzymatic anti-oxidants, such as SOD and GPx1³³. In a hyperglycemic state, there is an imbalance in the ROS : anti-oxidants ratio due to increased NADPH oxidase activity and decreased anti-oxidants, SOD and GPx1³⁴. Indeed, this was noted in the present study in an intermediate hyperglycemic state, which we postulate might have resulted in insulin resistance.

Previous studies in our laboratory have suggested that insulin resistance in the prediabetes state is directly proportional to increased ghrelin secretion³⁵. Through the orexigenic signaling pathway, ghrelin promotes high caloric intake, which has been proven to alter bodyweight³⁶. Therefore, in the current study, the caloric intake and bodyweights of the NPD and PD groups were measured at week 32, where the weights of the PD group were significantly higher than those in the NPD. In addition to the results of the present study, where we showed significantly higher plasma insulin concentration in the PD group, we have

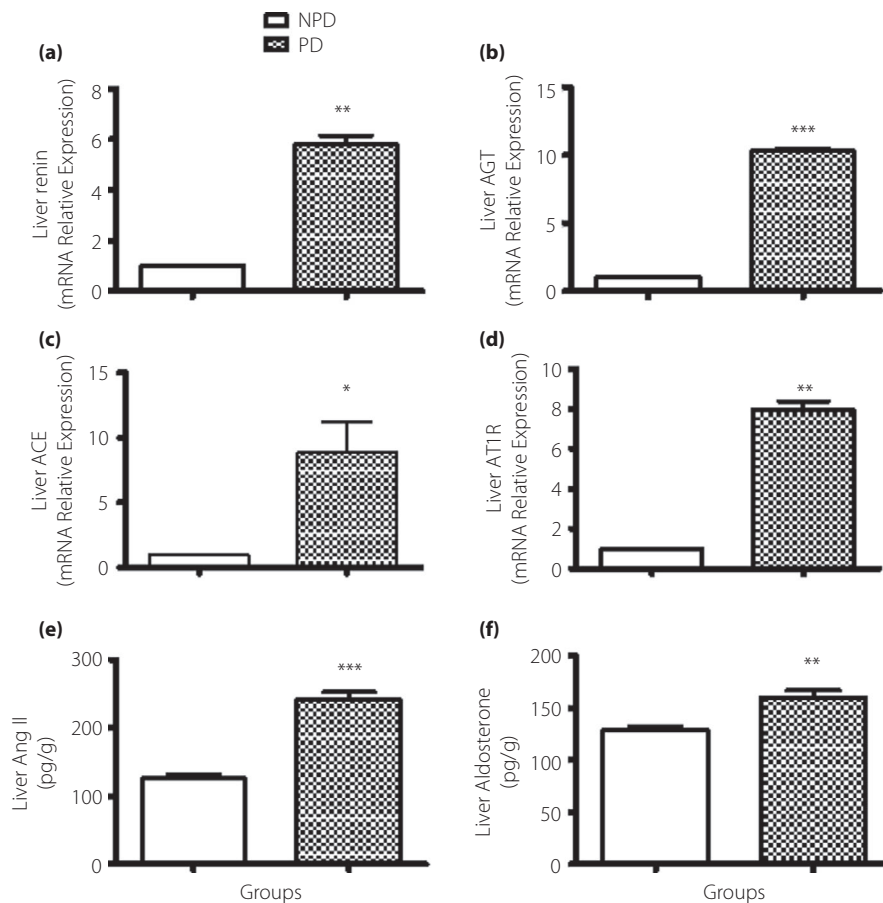


Figure 4 | The effects of a high-fat high-carbohydrate diet on the relative expression of the liver renin–angiotensin–aldosterone system components namely, (a) renin, (b) angiotensinogen (AGT), (c) angiotensin-converting enzyme (ACE) and (d) angiotensin II type 1 receptor (AT1R), and protein concentration of (e) angiotensin II (Ang II) and (f) aldosterone of rats at week 32. Values are presented as the mean \pm standard error of the mean. * $P < 0.05$, ** $P < 0.01$ and *** $P < 0.001$ denotes significance relative to the standard rat chow with normal drinking water (non-prediabetes [NPD]) diet-fed Male Sprague Dawley rats. mRNA, messenger ribonucleic acid; PD, prediabetes. (See the exact values for figure 4 in table 4.4 in the supplementary information)

also shown higher homeostasis model assessment of insulin resistance index scores in the PD group in comparison with the NPD group³⁵.

Due to impaired glucose tolerance associated with insulin resistance, glucose molecules bind to hemoglobin in red blood cells, thus resulting HbA1c³⁷. Accordingly, HbA1c was measured in the present study, whereby it was significantly higher in the PD group in comparison with the NPD group.

Insulin resistance has not only been shown in the skeletal muscle. Increasing evidence suggests that local RAAS also contributes to insulin resistance in the adipose tissue³⁸. The RAAS components have been reported to be highly expressed in the adipose tissue in hyperglycemia and type 2 diabetes³⁹. In the current study, renin, angiotensinogen, ACE, AT1R expression, Ang II and aldosterone were measured in the adipose tissue. Interestingly, the renin, angiotensinogen and AT1R expression was upregulated; however, there was no statistical difference

between the NPD and PD group in the ACE expression, Ang II and aldosterone concentration.

Local RAAS is physiologically essential in adipocyte differentiation and TG modulation⁴⁰. Mature adipocytes produce Ang II type 2 receptors, which facilitate mature insulin-sensitive adipocyte proliferation and preadipocyte differentiation, thus capacitating the insulin signaling pathway in addition to triglyceride metabolism and regulation^{41,42}. However, in a hyperglycemic state, due to the Ang II/AT1R signaling inducing the NADPH oxidase, the downstream effects result in insulin resistance⁴³. Although, in the current study, there was no significant difference between the NPD and PD group in the ACE expression, Ang II and aldosterone concentration. However, as a result of the increased expression of the AT1R, we might postulate there is increased Ang II/AT1R binding in the adipose tissue. The Ang II/AT1R binding in the adipose

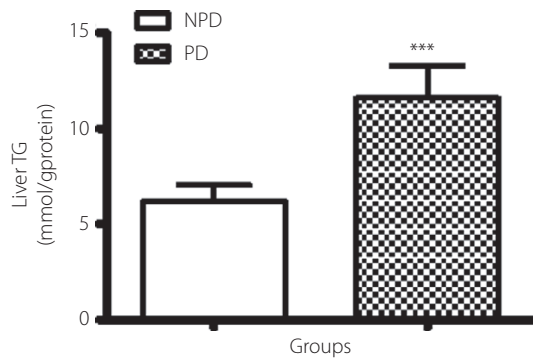


Figure 5 | The effects of a high-fat high-carbohydrate diet on the liver triglycerides (TG) concentration of rats at week 32. Values are presented as the mean \pm standard error of the mean. *** $P < 0.001$ denotes comparison with standard rat chow with normal drinking water (non-prediabetes [NPD]) diet-fed male Sprague–Dawley rats. PD, prediabetes. (See the exact numerical values for figure 5 in table 4.5 in the supplementary information)

has been evidenced to promote the generation of ROS through the upregulation of NADPH oxidase⁴⁴.

Additionally, the increased expression of the AT1R and decrease in Ang II type 2 receptors were noted in hyperglycemia results in lipodystrophy, a condition characterized by progressive loss or redistribution of fat⁴⁵. Lipodystrophy instigated by the Ang II/AT1R has been associated with a decrease in mature adipocytes that produce the Ang II type 2 receptors, which subsequently facilitate the differentiation of the insulin-sensitive preadipocytes⁴³. Hence, due to lipodystrophy, the upregulation of RAAS reduces the adipocyte lipid storage capacity and insulin sensitivity⁴³. This, therefore, leads to ectopic triglyceride relocation to other organs, such as the skeletal muscle, pancreas and liver, which was observed in the present study.

The liver, in addition to adipose tissue, facilitates lipid metabolism, whereby proteoglycans known as heparan sulfates are integral⁴⁶. In type 2 diabetes, due to hyperglycemia, RAAS components are upregulated, thus enabling Ang II/AT1R interactions, which impairs the ability of hepatic heparan sulfates to regulate lipid metabolism⁴⁷. Heparan sulfate's bioavailability is decreased in type 2 diabetes as a result of the reduced protein expression and enzymatic activity of N-deacetylase, which is a regulatory enzyme in hepatic heparan sulfate biosynthesis⁴⁸. These findings are consistent with the observations made in the present study, where there was a significant increase in liver TGs in the PD group when compared with the NPD group. We hypothesize that the upregulated RAAS components prompted by the moderate hyperglycemia in the present study enabled the Ang II/AT1R interaction in the liver. It then follows that the Ang II/AT1R interaction impaired the heparan sulfates synthesis by impeding the protein expression and enzymatic activity of N-deacetylase. Therefore, we speculate that the reduced bioavailability of heparan sulfates in the liver

resulted in impaired lipid metabolism, consequently promoting hyperlipidemia.

The elevated TGs in the liver instigate the process of gluconeogenesis, thus resulting in increased plasma glucose concentration⁴⁹. This is consistent with the significantly increased plasma glucose concentration in the current study. Furthermore, the pancreas is of paramount importance in glucose homeostasis due to the β -cells' ability to regulate glucose-mediated insulin secretion⁵⁰. Insulin deficiency has been associated with autoimmune destruction of the pancreatic β -cells noted in type 1 diabetes⁵¹. Interestingly, Robson-Doucette *et al.* observed a direct correlation between pancreatic RAAS activity in a hyperglycemic state and the hyperactivity of the pancreatic β -cells⁵². The upregulation of RAAS components, consequently Ang II/AT1R interaction in a hyperglycemia state, has been associated with impaired glucose-stimulated insulin secretion leading to glucotoxicity and lipotoxicity⁵³.

The Ang II/AT1R binding results in the upregulation of uncoupling-protein-2 (UCP-2), which facilitates the transfer of anions in exchange for protons from the inner to the outer mitochondrial membrane. Hence, UCP-2 regulates the mitochondrial membrane potential, which is dysregulated by the generation of ROS noted in hyperlipidemia and hyperglycemia⁵⁴. Obesity and type 2 diabetes are associated with an excess of nutrients, such as free fatty acids, which causes the upregulation of UCP-2, which in turn upregulates the key regulatory enzyme of β -oxidation, carnitine palmitoyltransferase I, thus generating ROS⁵². The upregulation of UCP is directly proportional to an excess in the generation of ROS and insulin insufficiency, because UCP does not only result in energy depletion, as it decreases adenosine triphosphate/adenosine diphosphate availability consequently, reducing glucose-stimulated insulin secretion^{55,56}. Furthermore, the increased expression of the UCP-2 induces apoptosis of the pancreatic β -cells, therefore, reducing β -cell density, hence reverberating insulin deficiency⁵⁶. Additionally, the upregulation of the Ang II/AT1R stimulates NADPH oxidase, causing an imbalance in the ROS and anti-oxidant ratio in favor of the ROS, consequently decreasing β -cell mass⁵⁷.

In the present study, there was no observable change in the ACE relative expression; therefore, the Ang II and aldosterone concentration remained constant in the PD group relative to the NPD group. However, due to significantly expressed AT1R, we could postulate that the Ang II/AT1R interaction was upregulated, which has been evidenced to instigate the generation of ROS, thus resulting in oxidative stress possibly due to the elevated NADPH oxidase and reduced anti-oxidants, which is indicative of local RAAS activity. The elevated Ang II/AT1R interaction promotes the generation of ROS through the NADPH oxidase activity, which has been shown to activate UCP-2⁵⁸. In the β -cells, the hyperactivity of UCP-2 promotes apoptosis of these cells, thus decreasing β -cell mass^{52,58}. Hence, the hyperactivity of UCP-2 in a hyperglycemic state has been suggested to be directly proportional to an increase in ROS and deficiency in insulin production in the pancreatic β -cells^{52,59}.

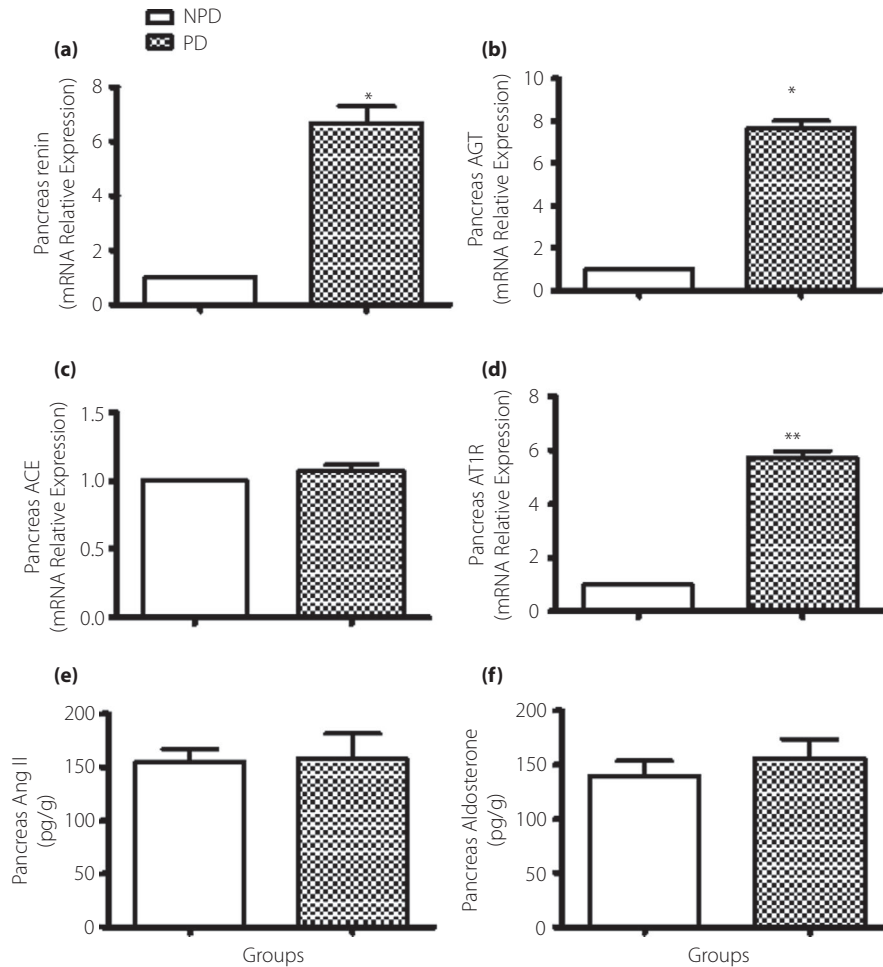


Figure 6 | The effects of a high-fat high-carbohydrate diet on the pancreas renin–angiotensin–aldosterone system components relative expression of (a) renin, (b) angiotensinogen (AGT), (c) angiotensin-converting enzyme (ACE) and (d) angiotensin II type 1 receptor (AT1R), and the protein concentration of (e) angiotensin II (Ang II) and (f) aldosterone of rats at week 32. Values are presented as the mean \pm standard error of the mean. * $P < 0.05$ and ** $P < 0.01$ denotes significance relative to the standard rat chow with normal drinking water (non-prediabetes [NPD]) diet-fed male Sprague–Dawley rats. mRNA, messenger ribonucleic acid; PD, prediabetes. (See the exact numerical values for figure 6 in table 4.6 in the supplementary information)

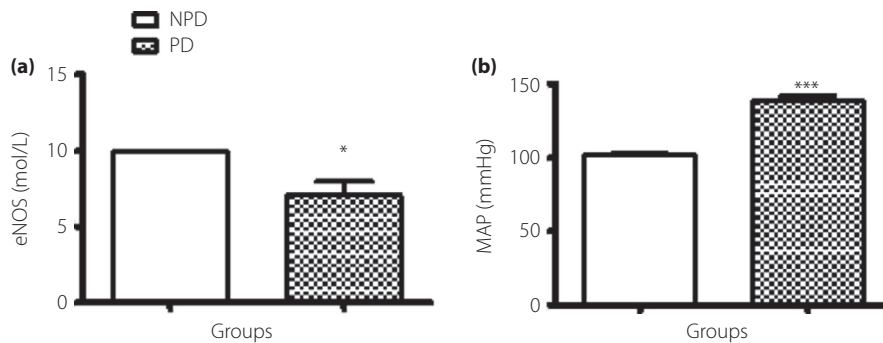


Figure 7 | Effects of ingesting a high-fat high-carbohydrate diet on (a) endothelial nitric oxide synthase (eNOS) and (b) mean arterial blood pressure (MAP) levels of rats at week 32. Values are presented as the mean \pm standard error of the mean. (a) * $P < 0.05$ and *** $P < 0.001$ denotes comparison with standard rat chow with normal drinking water (non-prediabetes [NPD]) diet-fed male Sprague–Dawley rats. PD, prediabetes. (See the exact numerical values for figure 7 in table 4.7 in the supplementary information)

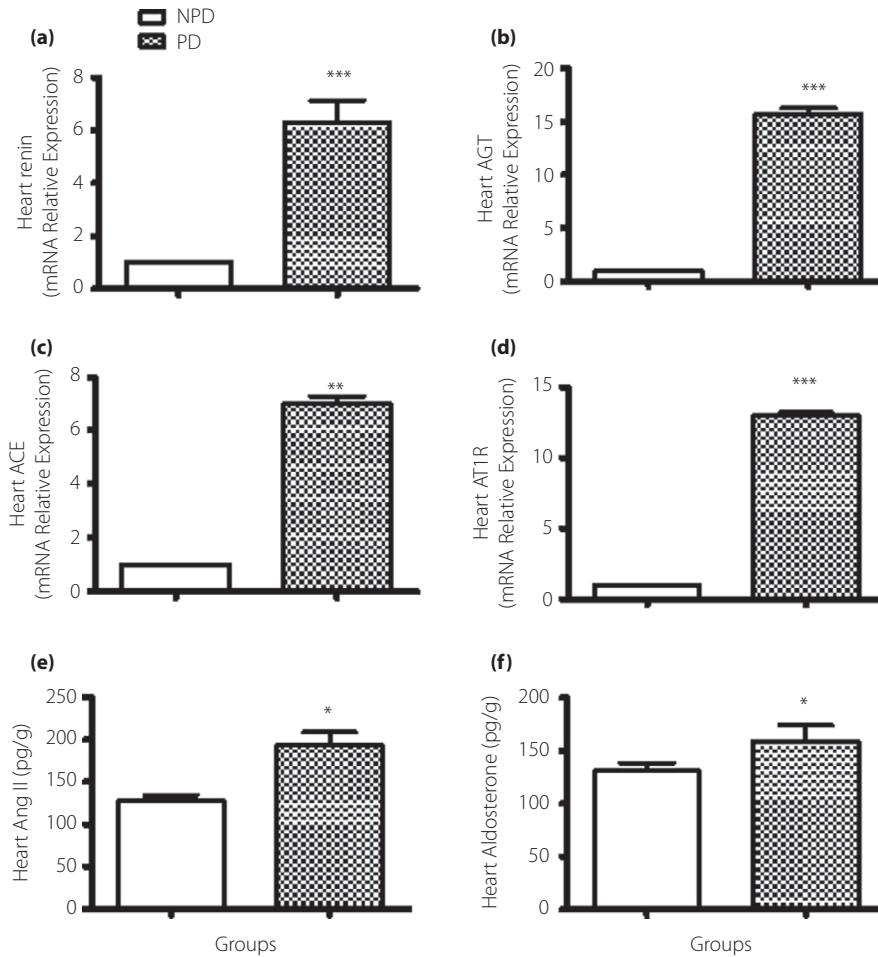


Figure 8 | The effects of a high-fat high-carbohydrate diet on the relative expression of the heart renin–angiotensin–aldosterone system components, namely, (a) renin, (b) angiotensinogen (AGT), (c) angiotensin-converting enzyme (ACE) and (d) angiotensin II type 1 receptor (AT1R) in addition to the protein concentration of angiotensin II (An II) and aldosterone of rats at week 32. Values are presented as the mean ± standard error of the mean. **P* < 0.05, ***P* < 0.01 and ****P* < 0.001 denotes significance relative to the standard rat chow with normal drinking water (non-prediabetes [NPD]) diet-fed male Sprague–Dawley rats. mRNA, messenger ribonucleic acid; PD, prediabetes. (See the exact numerical values for figure 8 in table 4.8 in the supplementary information)

TABLE 3 | Effect of diet-induced prediabetes on the oxidative stress markers nicotinamide adenine dinucleotide phosphate oxidase, superoxide dismutase and glutathione peroxidase 1 in male Sprague–Dawley rats

Tissues	NADPH oxidase (ng/L)		SOD (ng/mL)		GPx1 (pg/mL)	
	NPD	PD	NPD	PD	NPD	PD
Skeletal Muscle	400.8 ± 0.4	1211.0 ± 0.8**	8.6 ± 0.8	6.6 ± 0.6**	1693.9 ± 46.3	791.7 ± 40.1**
Pancreas	486.8 ± 0.3	601.5 ± 0.5*	2.7 ± 0.1	1.8 ± 0.1**	1422.2 ± 31.9	641.9 ± 42.3**
Heart	552.7 ± 0.3	899.4 ± 0.2**	8.5 ± 1.8	4.7 ± 1.2**	1813.4 ± 39.7	725.3 ± 48.6**

Values are presented as the mean ± standard error of the mean. **P* < 0.05 and ***P* < 0.01. GPx1, glutathione peroxidase 1; NADPH, nicotinamide adenine dinucleotide phosphate; NPD, non-pre-diabetes; PD, prediabetes; SOD, superoxide dismutase.

Interestingly, in the present study, although upregulation of the RAAS components and NADPH oxidase activity was observed in the PD group when compared with the NPD

group, the plasma insulin concentration was elevated. Therefore, as a result of the upregulated RAAS components, NADPH oxidase activity and decreased anti-oxidants in the pancreas, we

could suggest that RAAS is upregulated in the pancreas in pre-diabetes. Furthermore, we hypothesize that the significantly increased plasma insulin concentration is attributed to the compensatory mechanism of the β -cell suggested by Porat *et al.*, whereby the intact β -cells hyperfunction and consequently increase the plasma insulin concentration⁶⁰.

Insulin resistance in hyperglycemia has been linked to hyperinsulinemia and hypertension⁶¹. Insulin is integral in blood pressure homeostasis, as eNOS, the regulatory enzyme for nitric oxide (NO) synthesis, is the product of the insulin pathway⁶². The impairment of the insulin signaling pathway noted in type 2 diabetes has been associated with the upregulation of the RAAS and, consequently, hypertension due to the Ang II/AT1R binding impeding NO synthesis⁶³. Therefore, the plasma insulin concentration and mean arterial pressure in addition to plasma nitric oxide (eNOS) were analyzed in the present study. The plasma insulin concentration was increased, which could indicate hyperinsulinemia. Furthermore, the eNOS was significantly decreased, consequently decreasing NO. A decrease in NO, which is a potent vasodilator, causes an increase in blood pressure, which is consistent with the elevated mean arterial pressure observed in the present study.

A direct correlation between changes in systemic RAAS, hypertension and cardiac dysfunction has been established⁶⁴. In the past decade, RAAS has been characterized in the cardiac muscle, whereby the Ang II/AT1R binding contributes to the detrimental effects observed in type 2 diabetes, such as apoptosis, fibrosis and oxidative stress, through NADPH oxidase activity resulting in cardiac remodeling and hypertrophy⁶². Accordingly, in the present study, as a result of the significantly increased expression of the RAAS components, elevated NADPH oxidase and decreased anti-oxidants, we could suggest that the RAAS is upregulated, consequently contributing to cardiac remodeling and hypertrophy due to moderate hyperglycemia.

High caloric diets have been proven to promote the glycosylation of the P53 gene⁶⁵. Various studies have stressed the relationship between local RAAS and P53⁶⁵. Therefore, due to the high-fat high-carbohydrate diet, the glycosylation of P53 might be exacerbated and, consequently, local RAAS is upregulated. In view of the upregulated local RAAS in moderate hyperglycemia in the selected organs and the associated metabolic changes, we could postulate that the derangements observed in type 2 diabetes are a result of and begin in a prediabetes state.

ACKNOWLEDGMENTS

The authors thank Mr Makhubela for his technical assistance, the Biomedical Resource Unit employees, the University of KwaZulu-Natal for providing animals and the College of Health Sciences for their support. This work was supported by the College of Health Science of the University of KwaZulu-Natal and the National Research Foundation.

DISCLOSURE

The authors declare no conflict of interest.

Approval of the research protocol: The research protocol was approved by the University of KwaZulu Natal Animal Research Ethics Committee on 4 May 2018; ethics number: AREC/024/018D.

Informed consent: N/A.

Approval date of registry and the registration no. of the study/trial: N/A.

Animal studies: All animal experiments were approved by the University of KwaZulu Natal Animal Research Ethics Committee, which follows the national guidelines and the relevant national laws on the protection of animals.

REFERENCES

- Weir GC, Aguayo-Mazzucato C, Bonner-Weir S. β -cell dedifferentiation in diabetes is important, but what is it? *Islets* 2013; 5: 233–237.
- Marcus Y, Shefer G, Stern N. Adipose tissue renin–angiotensin–aldosterone system (RAAS) and progression of insulin resistance. *Mol Cell Endocrinol* 2013; 378: 1–14.
- Zhang J, Patel MB, Griffiths R, *et al.* Tumor necrosis factor- α produced in the kidney contributes to angiotensin II–dependent hypertension. *Hypertension* 2014; 64: 1275–1281.
- Briet M, Schiffrin EL. Aldosterone: effects on the kidney and cardiovascular system. *Nat Rev Nephrol* 2010; 6: 261.
- Williams LJ, Nye BG, Wende AR. Diabetes-related cardiac dysfunction. *Endocrinol and Metab* 2017; 32: 171–179.
- Remuzzi G, Perico N, Macia M, *et al.* The role of renin–angiotensin–aldosterone system in the progression of chronic kidney disease. *Kidney Int* 2005; 68: S57–S65.
- Lavoie JL, Sigmund CD. Minireview: overview of the renin–angiotensin system—an endocrine and paracrine system. *Endocrinology* 2003; 144: 2179–2183.
- Goossens G, Blaak E, Van Baak M. Possible involvement of the adipose tissue renin–angiotensin system in the pathophysiology of obesity and obesity-related disorders. *Obes Rev* 2003; 4: 43–55.
- de Zeeuw D, Remuzzi G, Parving H-H, *et al.* Proteinuria, a target for renoprotection in patients with type 2 diabetic nephropathy: lessons from RENAAL. *Kidney Int* 2004; 65: 2309–2320.
- Leung PS. The physiology of a local renin–angiotensin system in the pancreas. *J Physiol* 2007; 580: 31–37.
- Whiting DR, Guariguata L, Weil C, *et al.* IDF diabetes atlas: global estimates of the prevalence of diabetes for 2011 and 2030. *Diabetes Res Clin Pract* 2011; 94: 311–321.
- Agyemang C, Meeks K, Beune E, *et al.* Obesity and type 2 diabetes in sub-Saharan Africans—Is the burden in today's Africa similar to African migrants in Europe? The RODAM study. *BMC Med* 2016; 14: 166.

13. Frayn KN. Adipose tissue and the insulin resistance syndrome. *Proc Nutr Soc* 2001; 60: 375–380.
14. Ran J, Hirano T, Adachi M. Angiotensin II type 1 receptor blocker ameliorates overproduction and accumulation of triglyceride in the liver of Zucker fatty rats. *Am J Physiol Endocrinol Metab* 2004; 287: E227–E232.
15. Henriksen EJ. Improvement of insulin sensitivity by antagonism of the renin-angiotensin system. *Am J Physiol Regul Integr Comp Physiol* 2007; 293: 974–980.
16. Ruster C, Wolf G. Renin-angiotensin-aldosterone system and progression of renal disease. *J Am Soc Nephrol* 2006; 17: 2985–2991.
17. Restini CBA, Garcia AFE, Natalin HM, *et al.* Signaling Pathways of Cardiac Remodeling Related to Angiotensin II. In: Tolekova AN (ed), *Renin-Angiotensin System-Past, Present and Future*. IntechOpen, 2017.
18. Wu S, McCormick JB, Curran JE, *et al.* Transition from pre-diabetes to diabetes and predictors of risk in Mexican-Americans. *Diabetes Metab Syndr Obes* 2017; 10: 491.
19. Bansal N. Prediabetes diagnosis and treatment: a review. *World J Diabetes* 2015; 6: 296.
20. Luvuno M, Khathi A, Mabandla MVJSR. The effects of exercise treatment on learning and memory ability, and cognitive performance in diet-induced prediabetes animals. *Sci Rep* 2020; 10: 1–12.
21. Gamede M, Mabuza L, Ngubane P, *et al.* Plant-derived oleanolic acid ameliorates markers of subclinical inflammation and innate immunity activation in diet-induced pre-diabetic rats. *TAEM* 2020; 11: 2042018820935771.
22. Luvuno M, Khathi A, Mabandla M. Voluntary ingestion of a high-fat high-carbohydrate diet: a model for prediabetes. *PONTE Int Sci Res J* 2018; 74:119–143.
23. Gamede M, Mabuza L, Ngubane P, *et al.* Preventing the onset of diabetes-induced chronic kidney disease during prediabetes: the effects of oleanolic acid on selected markers of chronic kidney disease in a diet-induced prediabetic rat model. *Biomed Pharmacother* 2021; 139: 111570.
24. Mabuza L, Gamede M, Maikoo S, *et al.* Effects of a ruthenium schiff base complex on glucose homeostasis in diet-induced pre-diabetic rats. *Molecules* 2018; 23: 1721.
25. Furukawa H, Shinmura A, Tajima H, *et al.* Concentration of tissue angiotensin II increases with severity of experimental pancreatitis. *Mol Med Report* 2013; 8: 335–338.
26. Gamede M, Mabuza L, Ngubane P, *et al.* Plant-derived oleanolic acid ameliorates markers associated with non-alcoholic fatty liver disease in a diet-induced pre-diabetes rat model. *Diabetes Metab Syndr Obes* 2019; 12: 1953.
27. Joseph JJ, Echouffo Tcheugui JB, Effeo VS, *et al.* Renin-angiotensin-aldosterone system, glucose metabolism and incident type 2 diabetes mellitus: MESA. *J Am Heart Assoc* 2018; 7: e009890.
28. Chu KY, Leung PS. Angiotensin II in type 2 diabetes mellitus. *Curr Protein Pept Sci* 2009; 10: 75–84.
29. Underwood PC, Adler GK. The renin angiotensin aldosterone system and insulin resistance in humans. *Curr Hypertens Rep* 2013; 15: 59–70.
30. Goossens GH. The renin-angiotensin system in the pathophysiology of type 2 diabetes. *Obes Facts* 2012; 5: 611–624.
31. Sweeney EL, Jeromson S, Hamilton DL, *et al.* Skeletal muscle insulin signaling and whole-body glucose metabolism following acute sleep restriction in healthy males. *Physiol Rep* 2017; 5: e13498.
32. Diamond-Stanic MK, Henriksen EJ. Direct inhibition by angiotensin II of insulin-dependent glucose transport activity in mammalian skeletal muscle involves a ROS-dependent mechanism. *Arch Physiol Biochem* 2010; 116: 88–95.
33. Koju N, Taleb A, Zhou J, *et al.* Pharmacological strategies to lower crosstalk between nicotinamide adenine dinucleotide phosphate (NADPH) oxidase and mitochondria. *Biomed Pharmacother* 2019; 111: 1478–1498.
34. Volpe CMO, Villar-Delfino PH, dos Anjos PMF, *et al.* Cellular death, reactive oxygen species (ROS) and diabetic complications. *Cell Death Dis* 2018; 9: 119.
35. Siboto A, Akinnuga AM, Khumalo BN, *et al.* The effects of a [3+ 1] oxo-free rhenium (V) compound with uracil-derived ligands on selected parameters of glucose homeostasis in diet-induced pre-diabetic rats. *Obes Med* 2020; 19: 100258.
36. Beebe C. Body weight issues in preventing and treating type 2 diabetes. *Diabetes Spectr* 2003; 16: 261–266.
37. Borai A, Livingstone C, Abdelaal F, *et al.* The relationship between glycosylated haemoglobin (HbA1c) and measures of insulin resistance across a range of glucose tolerance. *Scand J Clin Lab Investig* 2011; 71: 168–172.
38. Saxena A, Tiwari P, Wahi N, *et al.* Transcriptome profiling reveals association of peripheral adipose tissue pathology with type-2 diabetes in Asian Indians. *Adipocyte* 2019; 8: 125–136.
39. Goossens GH, Moors CCM, van der Zijl NJ, *et al.* Valsartan improves adipose tissue function in humans with impaired glucose metabolism: a randomized placebo-controlled double-blind trial. *PLoS One* 2012; 7: e39930.
40. Cooper ME. The role of the renin-angiotensin-aldosterone system in diabetes and its vascular complications. *Am J Hypertens* 2004; 17: 16S–20S.
41. Than A, Xu S, Li RU, *et al.* Angiotensin type 2 receptor activation promotes browning of white adipose tissue and brown adipogenesis. *Signal Transduct Target Ther* 2017; 2: 17022.
42. Engeli S, Schling P, Gorzelniak K, *et al.* The adipose-tissue renin-angiotensin-aldosterone system: role in the metabolic syndrome? *Int J Biochem Cell Biol* 2003; 35: 807–825.
43. Ravussin E, Smith SR. Increased fat intake, impaired fat oxidation, and failure of fat cell proliferation result in ectopic fat storage, insulin resistance, and type 2 diabetes mellitus. *Ann N Y Acad Sci* 2002; 967: 363–378.

44. Den Hartigh LJ, Omer M, Goodspeed L, *et al.* Adipocyte-specific deficiency of NADPH oxidase 4 delays the onset of insulin resistance and attenuates adipose tissue inflammation in obesity. *Arterioscler Thromb Vasc Biol* 2017; 37: 466–475.
45. Wu C-H, Mohammadmoradi S, Thompson J, *et al.* Adipocyte (pro) renin-receptor deficiency induces lipodystrophy, liver steatosis and increases blood pressure in male mice. *Hypertension* 2016; 68: 213–219.
46. Werner A, Kuipers F, Verkade HJ. Fat absorption and lipid metabolism in cholestasis. In: Epstein FH (ed), *Molecular Pathogenesis of Cholestasis*. Waltham: The New England Journal Medicine; 2004:314–328.
47. MacArthur JM, Bishop JR, Stanford KI, *et al.* Liver heparan sulfate proteoglycans mediate clearance of triglyceride-rich lipoproteins independently of LDL receptor family members. *J Clin Invest* 2007; 117: 153–164.
48. Williams KJ, Liu M-L, Zhu Y, *et al.* Loss of heparan N-sulfotransferase in diabetic liver: role of angiotensin II. *Diabetes* 2005; 54: 1116–1122.
49. Jin ES, Browning JD, Murphy RE, *et al.* Fatty liver disrupts glycerol metabolism in gluconeogenic and lipogenic pathways in humans. *J Lipid Res* 2018; 59: 1685–1694.
50. Röder PV, Wu B, Liu Y, *et al.* Pancreatic regulation of glucose homeostasis. *Exp Mol Med* 2016; 48: e219.
51. Yoon J-W, Jun H-S. Autoimmune destruction of pancreatic β cells. *Am J Ther* 2005; 12: 580–591.
52. Robson-Doucette CA, Sultan S, Allister EM, *et al.* β -cell uncoupling protein 2 regulates reactive oxygen species production, which influences both insulin and glucagon secretion. *Diabetes* 2011; 60: 2710–2719.
53. Graus-Nunes F, Souza-Mello V. The renin-angiotensin system as a target to solve the riddle of endocrine pancreas homeostasis. *Biomed Pharmacother* 2019; 109: 639–645.
54. Yuan LI, Li X, Li J, *et al.* Effects of renin-angiotensin system blockade on the islet morphology and function in rats with long-term high-fat diet. *Acta Diabetol* 2013; 50: 479–488.
55. Newsholme P, Haber EP, Hirabara SM, *et al.* Diabetes associated cell stress and dysfunction: role of mitochondrial and non-mitochondrial ROS production and activity. *J Physiol* 2007; 583: 9–24.
56. Broche B, Ben Fradj S, Aguilar E, *et al.* Mitochondrial protein UCP2 controls pancreas development. *Diabetes* 2018; 67: 78–84.
57. Ramalingam L, Menikdiwela K, LeMieux M, *et al.* The renin angiotensin system, oxidative stress and mitochondrial function in obesity and insulin resistance. *Biochim Biophys Acta Mol Basis Dis* 2017; 1863: 1106–1114.
58. Affourtit C, Brand MD. On the role of uncoupling protein-2 in pancreatic beta cells. *Biochim Biophys Acta Mol Basis Dis* 2008; 1777: 973–979.
59. Liu J, Li JI, Li W-J, *et al.* The role of uncoupling proteins in diabetes mellitus. *J Diabetes Res* 2013; 2013: 1–7.
60. Porat S, Weinberg-Corem N, Tornovsky-Babaey S, *et al.* Control of pancreatic β cell regeneration by glucose metabolism. *Cell Metab* 2011; 13: 440–449.
61. Zhou M-S, Wang A, Yu H. Link between insulin resistance and hypertension: what is the evidence from evolutionary biology? *Diabetol Metab Syndr* 2014; 6: 12.
62. Zhou M-S, Schulman IH, Zeng Q. Link between the renin-angiotensin system and insulin resistance: implications for cardiovascular disease. *Vasc Med* 2012; 17: 330–341.
63. Symons JD, McMillin SL, Riehle C, *et al.* Contribution of insulin and Akt1 signaling to endothelial nitric oxide synthase in the regulation of endothelial function and blood pressure. *Circ Res* 2009; 104: 1085–1094.
64. Sharma AM. Is there a rationale for angiotensin blockade in the management of obesity hypertension? *Hypertension* 2004; 44: 12–19.
65. Fiordaliso F, Leri A, Cesselli D, *et al.* Hyperglycemia activates p53 and p53-regulated genes leading to myocyte cell death. *Diabetes* 2001; 50: 2363–2375.

SUPPORTING INFORMATION

Additional supporting information may be found online in the Supporting Information section at the end of the article.

Table S4 | Numerical values for all the figures included in the manuscript.